Annales Societatis Geologorum Poloniae (2023), vol. 93: 195–210 https://doi.org/10.14241/asgp.2023.05

CHROMIUM-RICH ILLITE/SMECTITE IN THE BASAL BALINKA CONGLOMERATE OF THE UPPER CARBONIFEROUS-PERMIAN BOSKOVICE BASIN (BOHEMIAN MASSIF)

Pavla HRŠELOVÁ[1, *], Stanislav HOUZAR[1], David BURIÁNEK[2], Dalibor VŠIANSKÝ[3], Marek SZCZERBA[5], Zuzanna CIESIELSKA[5], Jindřich ŠTELCL[3, 4] & Slavomír NEHYBA[3]

[1] *Department of Mineralogy and Petrography, Moravian Museum, Zelný trh 6, 659 37, Brno, Czech Republic; e-mails: phrselova@mzm.cz, shouzar@mzm.cz*
[2] *Czech Geological Survey, branch Brno, Leitnerova 22, 602 00 Brno, Czech Republic; e-mail: david.burianek@geology.cz*
[3] *Department of Geological Sciences, Faculty of Science, Masaryk University, Kotlářská 2, 611 37 Brno, Czech Republic; e-mails: dalibor@sci.muni.cz, stelcl@sci.muni.cz, slavek@sci.muni.cz*
[4] *Department of Biology, Faculty of Education, Masaryk University, Poříčí 7, 603 00 Brno, Czech Republic; e-mail: stelcl@sci.muni.cz*
[5] *Institute of Geological Sciences, Polish Academy of Sciences, Senacka 1, 31-002 Kraków, Poland; e-mails: m.szczerba@ingpan.krakow.pl, z.ciesielska@ingpan.krakow.pl*
** Corresponding author*

Hršelová, P., Houzar, S., Buriánek, D., Všianský, D., Szczerba, M., Ciesielska, Z., Štelcl, J. & Nehyba, S., 2023. Chromium-rich illite/smectite in the basal Balinka Conglomerate of the Upper Carboniferous-Permian Boskovice Basin (Bohemian Massif). *Annales Societatis Geologorum Poloniae*, 93: 195–210.

Abstract: The Upper Carboniferous polymictic Balinka Conglomerate was deposited along the western margin of the Boskovice Basin (eastern part of the Bohemian Massif). Angular aggregates of deep-green chromium-rich interstratified clay mineral R1-illite(0.8)/smectite (I/S) are present exclusively in the basal part of this unit. The textural position of chromium-bearing I/S (0.77–2.88 wt.% Cr_2O_3; 0.040–0.153 apfu Cr) in the conglomerate matrix indicates a genetic link with the highly altered chromium spinel, which is preserved in the relics. The source of Cr-rich spinelides was serpentinized peridotites in the adjacent Moldanubicum (Gföhl Unit). The formation of I/S is related to diagenetic processes in the conglomerate matrix. The fluids would have relatively high fugacity of CO_2 and activity of K^+. K/Ar ages of 284.1 ± 7.7 and 276.3 ± 7.4 Ma (lower Permian – Kungurian/Artinskian age) confirmed the diagenetic origin of this I/S.

Key words: Chromium illite-smectite, Cr-rich spinelides, Balinka Conglomerate, diagenetic alteration, Upper Carboniferous, Boskovice Basin, Bohemian Massif.

Manuscript received 15 June 2022, accepted 16 February 2023

INTRODUCTION

The depositional environment and climatic conditions significantly affect the composition of early diagenetic minerals (e.g., Burley *et al.,* 1985; Weibel *et al.,* 2017). Therefore, understanding the formation of new mineral phases in sediments is crucial for the interpretation of fluid–mineral diagenetic processes (e.g., Taylor *et al*., 2010). Cr-rich smectites can form by the decomposition of ultramafic and mafic rocks, as epigenetic minerals, filling voids left by the decomposition of organic matter in Permian sediments or filling material in cavities and fractures hosted by Pleistocene travertine and caliche (Foord *et al.*, 1987; Khoury, 2012; Khoury and Al-Zoubi, 2014; Mitsis *et al*., 2018).

The stability of the illite-smectite (I/S) group generally limits its environments of formation to near-surface settings (diagenesis, weathering), although it may precipitate in postmagmatic, low-grade metamorphic, and hydrothermal environments (Maksimovic and Brindley, 1980; Inoue *et al*., 2005; Manuella *et al.,* 2012). Sedimentary rocks contain I/S, originating from a range of source areas (Deocampo,

2015; Abbott *et al.,* 2019). However, chromium I/S in most cases is interpreted as the product of hydrothermal alteration of ultrabasic rocks (e.g., Maksimovic and Brindley, 1980).

In this work, the authors explored possible mechanisms of the formation of chromium-bearing I/S in the Balinka Conglomerate of the southern part of Boskovice Basin, Bohemian Massif. On the basis of an integrated approach, using X-ray diffraction, electron microscopy and microprobe analyses, the authors investigated the mechanism of formation of chromium-rich I/S after spinel. The discovery of this chromium-bearing phyllosilicate (Houzar *et al.*, 2013, 2017) in the Upper Carboniferous–Lower Permian sediments and their K/Ar dating provide precise information about the timing of diagenetic processes in the Boskovice Basin.

THE BOSKOVICE BASIN – GEOLOGICAL SETTING

The Boskovice Basin (BB) is situated in the eastern part of the Bohemian Massif at the boundary between the Moldanubian zone, the Bohemicum, and the Moravosilesian zone (Čepek, 1946; Jaroš, 1961). Sedimentation in this postorogenic intracontinental basin was controlled by a major NNE-trending marginal dextral strike-slip fault (Čepek, 1946; Jaroš, 1961). The Carboniferous-Permian sedimentary succession is a cyclic alternation of fluvial and limnic sediments (sandstones, mudstones, conglomerates, and subordinate bituminous and carbonate-rich sediments). The current width of the Boskovice Basin is 5 to 12 km and the length approximately 90 km (Fig. 1). The maximum present-day thickness of the Boskovice Basin sedimentary fill is assumed to be less than 3,000 m (Šimůnek and Martínek, 2009).

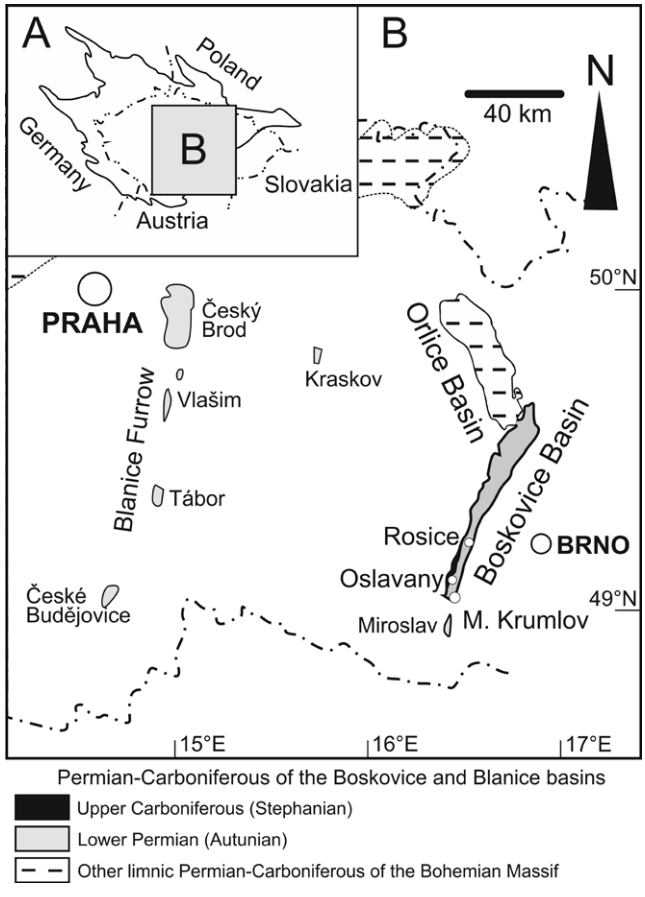

Fig. 1. Position of the Boskovice Basin in the eastern part of the Bohemian Massif and its relation to limnic Permian-Carboniferous sediments. The study area lies between Rosice and M. Krumlov (see Fig. 2).

The basin depocentre is divided into the southern Rosice-Oslavany Sub-basin and the northern Letovice Sub-basin (Havlena, 1964; Pešek *et al.,* 2001). In the older southern sub-basin (Fig. 2), the sedimentation (Stephanian C – lower Autunian = late Ghzelian – early Asselian) started by the Balinka and Rokytná conglomerates, followed by deposits of the Rosice-Oslavany and Padochov formations. Younger (lower–middle Autunian = Asselian) deposits of the Veverská Bítýška and Letovice formations fill the northern sub-basin (Pešek *et al*., 2001; Pešek, 2004). There are two types of thick conglomerate sequence, produced by the accumulation of alluvial fan deposits along the margin of Boskovice Basin. The Rokytná Conglomerate evolved along the tectonically active eastern basin margin (Main Fault of the Boskovice Basin), whereas the Balinka Conglomerate is situated along the western margin.

Scarce volcanic activity is recorded mainly in the Rosice-Oslavany Sub-basin. Dacites, andesites, trachyandesites, and basalts in the Boskovice Basin were described as dykes that cut sediments of the Rosice-Oslavany and Padochov Formation (Přichystal, 1993, 1994). Acid volcaniclastic rocks are present as up to 50 cm layers in the Rosice-Oslavany formations (Králík and Malý, 1987). U-Pb geochronology on single zircon crystals from a layer of volcaniclastic rocks near the top of the Rosice-Oslavany Formation provided an age of 298.88 ± 0.09 Ma (Opluštil *et al.,* 2017).

The study area (Fig. 2) is situated along the western edge of the Rosice-Oslavany Sub-basin between Rakšice near Moravský Krumlov and Oslavany (Havírna-Balinka). The basal Balinka Conglomerate here is covered by sandstones and mudstones of the Rosice-Oslavany and Padochov formations.

The Balinka Conglomerate (Suess, 1907) in the study area is a basal member of the coal-bearing Rosice-Oslavany Formation (Upper Carboniferous). It is separated from the underlying crystalline rocks by a sharp and irregular base, usually a few metters thick and may show upward and lateral transitions into arkosic sandstones (Jaroš, 1961). It may be locally developed as breccia at the base with a rapid upward transition into the predominant conglomerate, which indicates that weathering and talus slope development were simultaneous with the early stages of alluvial fan sedimentation (Went, 2005).

Dominant angular clasts (paragneisses, orthogneisses, migmatites, mica-schists, phyllites, quartzites, and quartz) originated from nearby geological units. Granulites, aplites, marbles, pyrope- and talc-rich serpentinites are rare (<4%). The rounded to angular and subangular pebbles reveal either longer transport duration with a greater role of stream flows or they indicate redeposition (Hršelová *et al.,* 2021). The matrix consists of quartz and K-feldspars, Na-rich

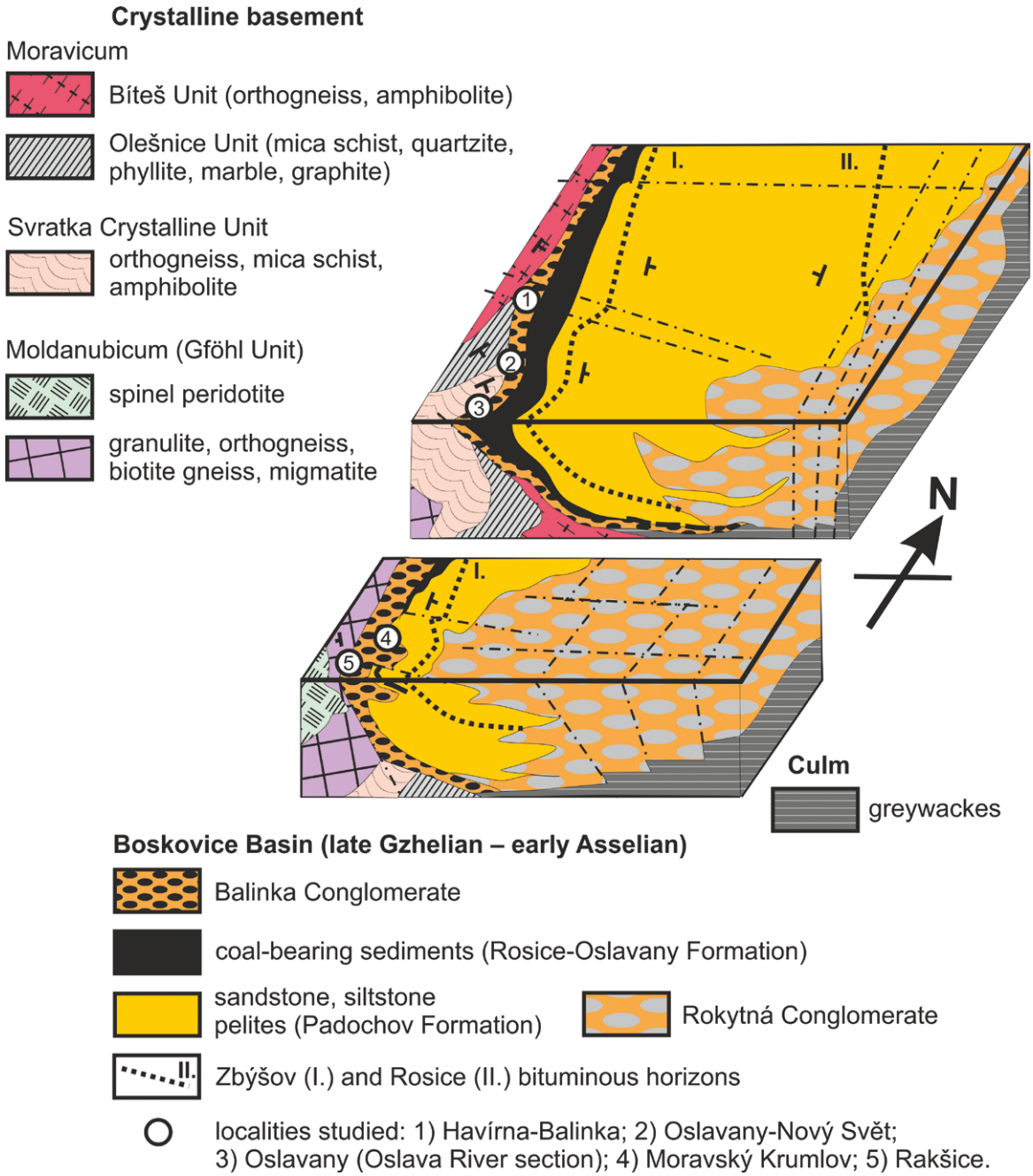

Fig. 2. Geological situation in the southern part of the Boskovice Basin with position of the studied localities (modified according to Malý, 1993).

plagioclases, strongly chloritized and hematitized biotite, muscovite, illite/smectite, and clasts of metamorphosed, sedimentary, and igneous rocks. The heavy mineral association (> 0.10 mm) consists of variable amounts of garnet, zircon, tourmaline, Cr-rich spinelides, magnetite, and ilmenite (Hršelová *et al.,* 2018, 2021).

Similar conglomerate also occurs in several higher horizons in the Upper Carboniferous coal-bearing psammitic sedimentary sequence (Malý and Uhrová, 1962, 1980). The Balinka Conglomerate is completely devoid of fossils.

The Upper Carboniferous Rosice-Oslavany Formation (Havlena, 1964; Opluštil *et al.,* 2016) consists of red to grey sandstones and mudstones with various intercalations of the Balinka Conglomerate lithotype, coal-bearing mudstones, coal, and volcaniclastic rocks (Šimůnek and Martínek, 2009; Opluštil *et al.,* 2017).

The overlying brown-red sandstones, arkoses, and aleuropelites of the Padochov Formation (lower Permian) form the dominant lithofacies of the subbasin. Grey pelites, sporadic micritic limestones, and some bituminous shales or marls are rich in fossils (Zbýšov and Rosice horizons, Opluštil *et al.,* 2017).

Representative conglomerates were collected from outcrops of the Balinka Conglomerate with a specific horizon, where the green I/S aggregates are clearly present. The studied samples are oligomictic, well-cemented, matrix-supported conglomerates. The locations of the collection points are shown in Table 1.

Table 1

Position of the studied localities and the underlying rock types.

Locality	Latitude	Longitude	Underlying rock types
1. Havírna-Balinka	49°7′57.881″N	16°19′59.901″E	mica schists, fine-grained gneisses, orthogneiss
2. Nový Svět	49°8′25.122″N	16°20′13.960″E	mica schists
3. Oslavany	49°7′41.971″N	16°20′3.271″E	pink orthogneiss, mica schist
4. Moravský Krumlov	49°3′2.948″N	16°18′25.089″E	unknown
5. Rakšice	49°2′17.739″N	16°17′57.965″E	pink orthogneiss, serpentinite

METHODS

Locality study and sample preparation

The Balinka Conglomerate was investigated macroscopically and in thin sections for the composition of the pebble fractions (8–64 mm; 100 fragments from the area of 1 m^2) and the matrix. Special attention was paid to chromium-containing phyllosilicates and accessory heavy minerals. Heavy minerals (HM) were separated from 10 kg of conglomerates by mechanical disintegration, sieving, and separation in acetylenetetrabromide (density 2.964 g/cm^3 at 20 °C). Rock forming minerals were studied, both in thin section and polished epoxy mount.

Electron-probe microanalysis (EPMA)

EPMA measurements were performed with a Cameca SX-100 instrument at the Joint Laboratory of Electron Microscopy and Microanalysis of Masaryk University and the Czech Geological Survey (Brno, Czech Republic). The measurements were carried out in a wavelength-dispersive mode under the following conditions: accelerating voltage 15 kV, beam current 10 nA or 20 nA; beam diameter of 1 or 4 μm. The standards, X-ray lines, monochromators, counting times and detection limits used for phyllosilicates analysis are shown in Table 2. The raw data were corrected, using the PAP correction (Pouchou and Pichoir, 1985). The abbreviations of the mineral names, used in the text, are according to Whitney and Evans (2010).

X-ray powder diffraction (XRPD)

Mechanically separated green coatings of samples, collected at five sites (Havírna-Balinka, Nový Svět, Oslavany, Moravský Krumlov, and Rakšice) were gently ground with mortar and pestle, dispersed in distilled water in 12 ml plastic test tubes and subjected to repeated ultrasonic disintegration and centrifugation. Three fractions of each sample were prepared and oriented mounts were created of them: < 2 μm, < 5 μm and the remaining coarse fraction (> 5 μm). The fraction < 2 μm was obtained in suspension by 750 rpm centrifugation for 3.3 min. The excess suspension was decanted. The same sample was dispersed in water again and centrifuged at 300 rpm for 3.3 min to obtain the particle size < 5 μm. The excess suspension was decanted again. The coarse > 5 μm sedimented fraction was pulverised in distilled water using a McCrone Micronising Mill and dispersed in a larger amount of water to create oriented mounts. The preparation of < 2 and < 5 μm fractions was carried out according to the Jackson procedure (1979) described by Moore and Reynolds (1997). Oriented specimens were prepared on zero background silicon wafers and were primarily used to identify clay minerals.

The XRPD analysis was conducted using a Panalytical X´Pert MPD PRO instrument with RTMS detector (X'Celerator) and Fe-filtered Co radiation ($\lambda_{Kα1}$ = 0.178901 nm) at Bragg-Brentano reflection geometry. The tube was powered at 40 kV and 30 mA. 2Θ range: 3.7–50 °2Θ for oriented mounts, step size: 0.033 °2Θ, time per step: 150 s, total scan duration: 1712 s. The analysis of oriented specimens was performed after three procedures: 1) air-drying, 2) saturation with ethylene glycol and 3) heating to 375 °C for 1 h. The data were processed with the Panalytical High Score 3 plus and Bruker AXS Diffrac plus EVA 2 software. ICDD PDF-2 and ICSD 2012 databases were used.

Ordering type (Reichweite) of illite/smectite was determined by the position of 002/003 reflection in EG treated samples (Jagodzinski, 1949). The illite content was estimated on the basis of the Δ2Θ value of 001/002 and 002/003 reflections (Moore and Reynolds, 1997).

K-Ar dating

Two samples (i.e., Oslavany and Rakšice) were dated by the K-Ar method. The potassium contents were measured, using a Sherwood Model 420 flame photometer. Radiogenic argon measurements were performed on an Nu Instruments Noblesse multicollector noble-gas spectrometer. The tantalum foil-wrapped portions were melted by defocused 972 nm infrared laser in a vacuum preparatory line. Gases extracted from the samples were cleaned by a titanium sublimation getter and then by two getter pumps. All the samples were melted for the second time, using the same procedure of measurement, but with a higher laser power. Pure ^{38}Ar was used as the spike. The amount of the original aliquot of ^{38}Ar spike was determined by measuring the international standard GLO (Odin, 1982), which are measured several times with every batch of samples. Age errors were calculated from the law of error propagation, taking into account the uncertainties of spectrometric measurement of argon isotopes, weighting, potassium measurements, normalization of amount of ^{38}Ar in spike based on dating of the GLO

Table 2

Standards, X-ray lines, monochromators, counting times and detection limits used for phyllosilicates analysis.

Element	X-ray	Monochormator	Standard	Counting time [s] peak/background	Detection limit [ppm]
F	*K*α	PC1	topaz	20 / (2 × 10)	760
Na	*K*α	TAP	albite	10 / (2 × 5)	701
Mg	*K*α	TAP	Mg_2SiO_4	20 / (2 × 10)	317
Si	*K*α	TAP	wollastonite	10 / (2 × 5)	515
Al	*K*α	TAP	sanidine	10 / (2 × 5)	365
K	*K*α	PET	sanidine	20 / (2 × 10)	401
Ca	*K*α	LPET	wollastonite	20 / (2 × 10)	315
Ti	*K*α	LPET	anatase	20 / (2 × 10)	229
Cr	*K*α	LPET	chromite	20 / (2 × 10)	228
V	*K*α	LLIF	ScVO4	20 / (2 × 10)	442
Mn	*K*α	LLIF	spessartine	20 / (2 × 10)	502
Fe	*K*α	LLIF	almandine	10 / (2 × 5)	740
Ni	*K*α	LLIF	Ni_2SiO_4	20 / (2 × 10)	486

standard and assessment of $^{40}Ar/^{36}Ar$ and $^{40}Ar/^{38}Ar$ ratios, measured every day for air aliquots.

RESULTS

Several minerals with an increased Cr content were found in the matrix of the Balinka Conglomerate. The most important of these are angular green I/S aggregates, in which relics of Cr–rich spinelides (magnesiochromite, chromite and chromspinel) are located.

Chromium-rich illite/smectite and chlorite

Chromium-rich I/S forms intensive green irregular massive aggregates (Fig. 3), 5–20 mm in size. Relics of disintegrated and etched Cr–rich spinelides were also determined in several chromium I/S aggregates (Fig. 4B–D). The places for the determination of I/S composition were thoroughly checked in BSE, spots with a sufficiently large area of I/S without the visible presence of submicron admixture of spinelides were selected.

The chemical composition (Tab. 3) of the phyllosilicates studied is similar to that of dioctahedral mica, with the general formula $I\ M_{2-3}\ \square_{1-0}\ T_4O_{10}\ A_2$, which includes micas deficient in dioctahedral interlayer (I) of the illite group (Rieder *et al.*, 1998).

Illite/smectite is close to the illite series nominal formula $K_{0.65}Al_{2.0}Al_{0.65}Si_{3.35}O_{10}\ (OH)_2$, with octahedral cation ratio $^{VI}R^{2+}/(^{VI}R^{2+}+\ ^{VI}R^{3+}) \leq 0.25$; $^{VI}Al/(^{VI}Al+\ ^{VI}Fe^{3+}) \geq 0.6$ and the total of I cations 0.6–0.85 (Fig. 5A; Rieder *et al.,* 1998). The detailed study of Środoń et al. (2009) defined the chemical composition of pure illite: $FIX_{0.95}(Si_{3.25}Al_{0.75})(Al_{1.81}Fe_{0.01}Mg_{0.19})O_{10}(OH)_2$.

Potassium (6.08–8.01 wt.% K_2O; 0.508–0.698 apfu K) predominates over Ca (0.025–0.071 apfu) and Na (≤ 0.012 apfu) in the I/S from the Balinka Conglomerate. The Al amount varies from 23.16 to 28.21 wt.% Al_2O_3. Aluminum dominates at the octahedral position M (1.335–1.627 apfu Al). There is usually more Mg (0.162–0.404 apfu) than Fe^{2+} (0.137–0.327 apfu) in I/S. The Cr_2O_3 contents vary between 0.77–2.88 wt.% (0.040–0.153 apfu Cr). The contents of Mn (≤0.003 apfu), V (≤0.005 apfu), Ni (≤0.008 apfu), and Ti (≤0.006 apfu) are below or close to the detection limit. The tetrahedral sheet contains 3.391–3.541 apfu Si and 0.459–0.609 apfu Al. The A-position (OH) accommodates a small proportion of F (0.034–0.139 apfu). Representative results of EPMA measurements are presented in Table 3.

Careful observation on BSE, in combination with EDS and WDS chemical microanalysis, revealed the local presence of Cr-bearing chlorite in a mixture with I/S. Chemical analysis of chromium-bearing chlorite indicated chemical variations, mostly in terms of Cr_2O_3 (2.92–0.01 wt.%) and FeO_{tot} (17.27–27.14 wt.%). The presence of interlayer cations, such as Na, K and Ca (max. 0.69 apfu) in the chemical data, could be explained by the existence of a mixture of phases between chromium I/S and chlorite, causing compositional variations like those described by Morata *et al.* (2001) or Do Campo and Nieto (2005).

Phase analysis and identification of I/S structure

The dominant component of the studied samples in all separated fractions is interstratified clay mineral R1-illite (0.8)/smectite. It was identified on the basis of Méring´s principle (Méring, 1949), using oriented mounts (Figs 6, 7; Suppl. Figs 1–4). The broad basal reflection with a maximum at 11.3–11.4 Å in air dried samples, which splits between 12.1–12.5 Å and 9.5–9.6 Å reflections after EG treatment may be assigned to (001)illite/(001)EG-smectite and (001)illite/(002)EG-smectite, respectively. The 5.01(2)

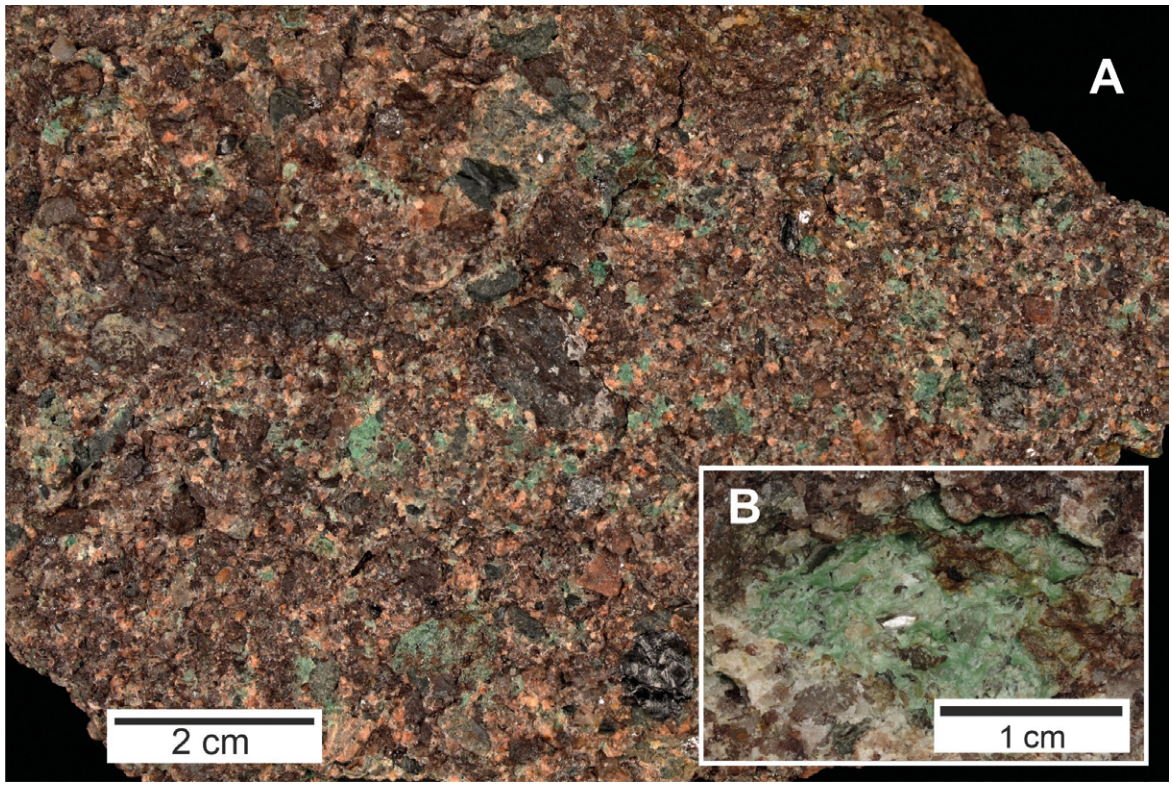

Fig. 3. Balinka Conglomerate; locality Oslavany. **A.** Green chromium-rich illite/smectite aggregates together with light K-feldspar clasts in the matrix of the conglomerate. **B.** Macrophotography of I/S aggregate filling the cavities between clasts in the Balinka Conglomerate. Photograph by J. Cága and R. Kummer.

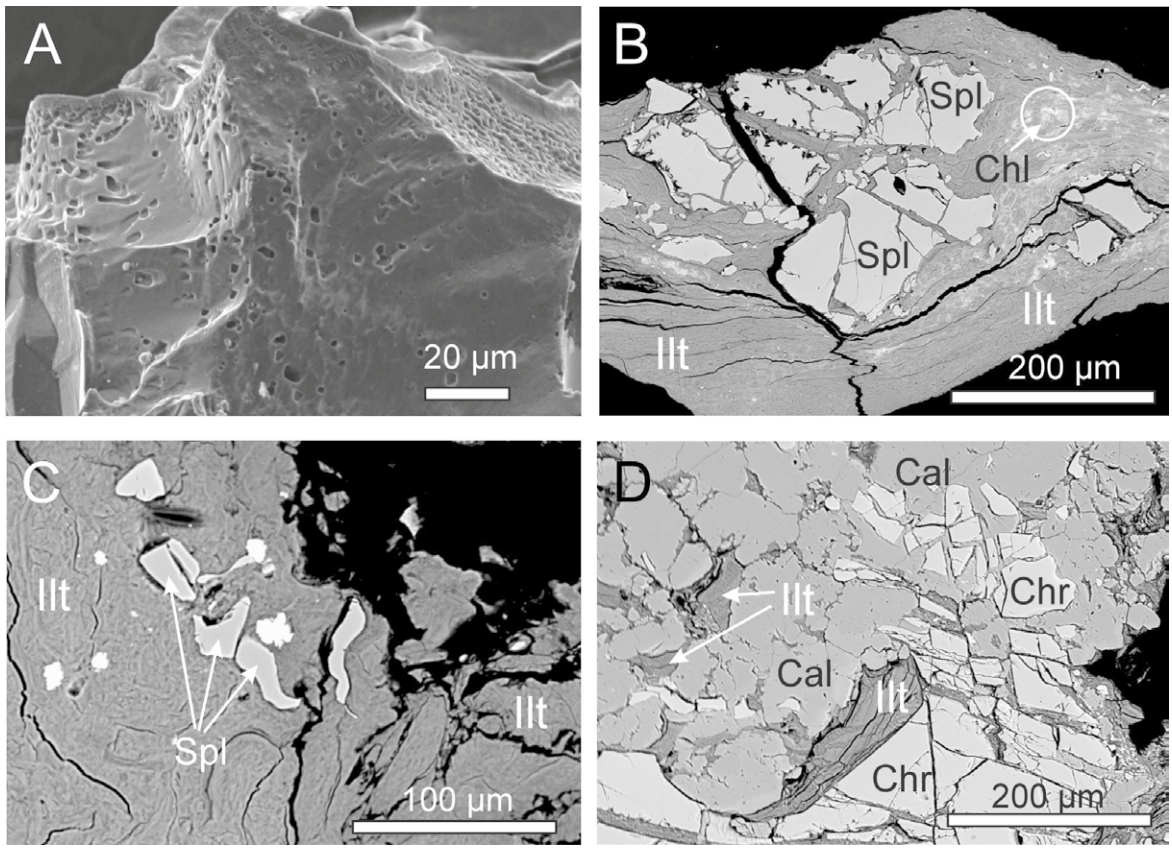

Fig. 4. Microstructural relationships between newly formed and original minerals. **A.** An isolated chromium spinel grain with etch pits on the surface (Oslavany). **B.** Cr-spinel (Spl) replaced by chromium I/S (Ilt) and chlorite (Chl) (Nový Svět). **C.** Anhedral relic Cr-spinel enclosed in chromium I/S (Rakšice). **D.** Chromite (Chr) with chromium I/S and calcite (Nový Svět).

Table 3

Representative results of EPMA measurements of Cr-rich illite.

	71ra	72ra	47ba	80ns	79ns	55os	60mk	57mk	2os	64ra	1ba	2ba
wt.%												
SiO_2	52.05	52.62	53.46	52.02	52.54	52.62	52.54	52.77	52.52	53.34	52.76	50.21
TiO_2	0.05	0.02	0.06	0.09	0.04	0.03	0.03	0.03	b.d.	0.02	b.d.	0.12
Al_2O_3	23.16	23.55	24.95	24.70	24.99	26.19	26.22	27.81	27.74	27.90	28.21	26.62
Cr_2O_3	2.88	2.25	2.09	1.96	1.76	1.43	1.14	1.06	0.89	0.77	1.37	2.41
V_2O_3	0.05	0.06	0.09	0.04	0.04	b.d.	0.03	0.01	0.06	b.d.	b.d.	b.d.
NiO	0.02	b.d.	b.d.	0.02	0.08	b.d.	b.d.	b.d.	b.d.	0.08	0.15	0.02
FeO	4.33	4.51	4.55	5.85	5.07	3.76	4.90	3.22	2.91	2.54	2.50	5.02
MnO	0.03	0.05	0.05	0.04	b.d.	0.01	0.03	b.d.	b.d.	0.02	0.01	0.02
MgO	4.03	3.38	2.39	2.40	2.21	2.32	1.97	2.22	2.02	3.14	3.05	1.61
CaO	0.98	0.93	0.39	0.94	0.87	0.86	0.84	0.89	0.97	0.65	0.36	0.51
Na_2O	0.01	0.06	0.03	0.09	0.04	0.06	0.06	0.04	b.d.	0.03	0.05	0.02
K_2O	6.69	7.50	7.80	7.36	7.55	7.78	7.59	7.48	7.99	6.93	6.08	8.10
F	0.20	0.25	0.20	0.16	0.18	0.22	0.19	0.20	0.21	0.37	0.67	0.22
H_2O*	4.36	4.35	4.43	4.41	4.41	4.42	4.43	4.48	4.45	4.43	4.26	4.34
O=F	-0.08	-0.11	-0.08	-0.07	-0.08	-0.09	-0.08	-0.08	-0.09	-0.16	-0.28	-0.09
TOTAL	98.76	99.42	100.41	100.01	99.70	99.61	99.89	100.13	99.67	100.06	99.19	99.13
apfu												
Si^{4+}	3.500	3.528	3.541	3.478	3.507	3.490	3.487	3.460	3.463	3.472	3.452	3.391
$^{(IV)}Al^{3+}$	0.500	0.472	0.459	0.522	0.493	0.510	0.513	0.540	0.537	0.528	0.548	0.609
$^{(VI)}Al^{3+}$	1.335	1.389	1.489	1.424	1.473	1.537	1.538	1.609	1.619	1.613	1.627	1.510
Cr^{3+}	0.153	0.119	0.109	0.104	0.091	0.075	0.060	0.055	0.046	0.040	0.071	0.129
Ti^{4+}	0.003	0.001	0.003	0.005	0.002	0.001	0.001	0.001		0.001		0.006
V^{3+}	0.003	0.003	0.005	0.002	0.002		0.002	0.001	0.003			
Ni^{2+}	0.001			0.001	0.004					0.004	0.008	0.001
Fe^{2+}	0.243	0.253	0.252	0.327	0.283	0.209	0.272	0.177	0.160	0.138	0.137	0.284
Mn^{2+}	0.002	0.003	0.003	0.002		0.001	0.002			0.001	0.001	0.001
Mg^{2+}	0.404	0.338	0.236	0.239	0.220	0.229	0.195	0.217	0.199	0.305	0.298	0.162
Ca^{2+}	0.071	0.067	0.028	0.067	0.062	0.061	0.060	0.063	0.069	0.045	0.025	0.037
Na^{+}	0.001	0.008	0.004	0.012	0.005	0.008	0.008	0.005		0.004	0.006	0.003
K^{+}	0.574	0.603	0.598	0.628	0.643	0.658	0.643	0.626	0.672	0.576	0.508	0.698
F^{-}	0.043	0.053	0.042	0.034	0.038	0.046	0.040	0.041	0.044	0.076	0.139	0.047
H^{+}	1.957	1.947	1.958	1.966	1.962	1.954	1.196	1.959	1.956	1.924	1.861	1.953
O^{2-}	11.957	11.947	11.958	11.966	11.962	11.954	11.960	11.959	11.956	11.924	11.861	11.953
CAT SUM	8.747	8.731	8.685	8.777	8.747	8.733	7.977	8.713	8.724	8.651	8.542	8.784
AN SUM	12	12	12	12	12	12	12	12	12	12	12	12

Notes: ba – Havírna-Balinka, ns – Nový Svět, os – Oslavany, mk – Moravský Krumlov, ra – Rakšice. b.d. – bellow detection.
* Structural formulae were calculated by normalizing cation analyses to a theoretical structure containing $O_{10}(OH)_2$

Å reflection (air-dried) splits into 5.19 Å [(002)illite/(003) EG-smectite] and 4.75 Å [(002)illite/(004)EG-smectite] reflections after EG treatment. The broad reflection at ca. 3.3 Å (air-dried) shifts to 3.33–3.35 Å after EG-treatment and may be assigned to (003)illite/(005)EG-smectite here. I/S identification was confirmed by heating to 375 °C for 1 hour leading to collapse of smectite layers and the result was a diffraction pattern similar to illite (Moore and Reynolds, 1997). Only insignificant differences in the illite/smectite structure of the examined samples were found. The R1-ordering type (Reichweite) of I/S, determined by the position of 002/003 reflection in ethylene glycol treated samples, is the same for all of the localities. The illite content in I/S estimates, based on the $\Delta 2\Theta$ value of 001/002 and 002/003 reflections (Moore and Reynolds, 1997), reaches ca. 80% (Tab. 4).

Table 4

Position of the basal reflections of illite/EG-smectite used for illite in I/S percentage estimation.
Diffractograms were measured with Co radiation, the reflection values for commonly used $Cu_{K\alpha 1}$ were calculated.

Sample	$(001)_I/(002)_{EG-S}$			$(002)_I/(003)_{EG-S}$			Δ °2Θ ($CuK\alpha_1$)	Ordering type	Illite (%)
	d(Å)	°2Θ ($CoK\alpha_1$)	°2Θ ($CuK\alpha_1$)	d(Å)	°2Θ ($CoK\alpha_1$)	°2Θ ($CuK\alpha_1$)			
Havírna-Balinka	9.54	10.76	9.26	5.19	19.85	17.07	7.81	1	80
Oslavany	9.54	10.76	9.26	5.19	19.85	17.07	7.81	1	80
M. Krumlov	9.67	10.62	9.14	5.19	19.85	17.07	7.93	1	82
Nový Svět	9.63	10.66	9.18	5.19	19.85	17.07	7.89	1	81
Rakšice	9.63	10.66	9.18	5.19	19.85	17.07	7.89	1	81

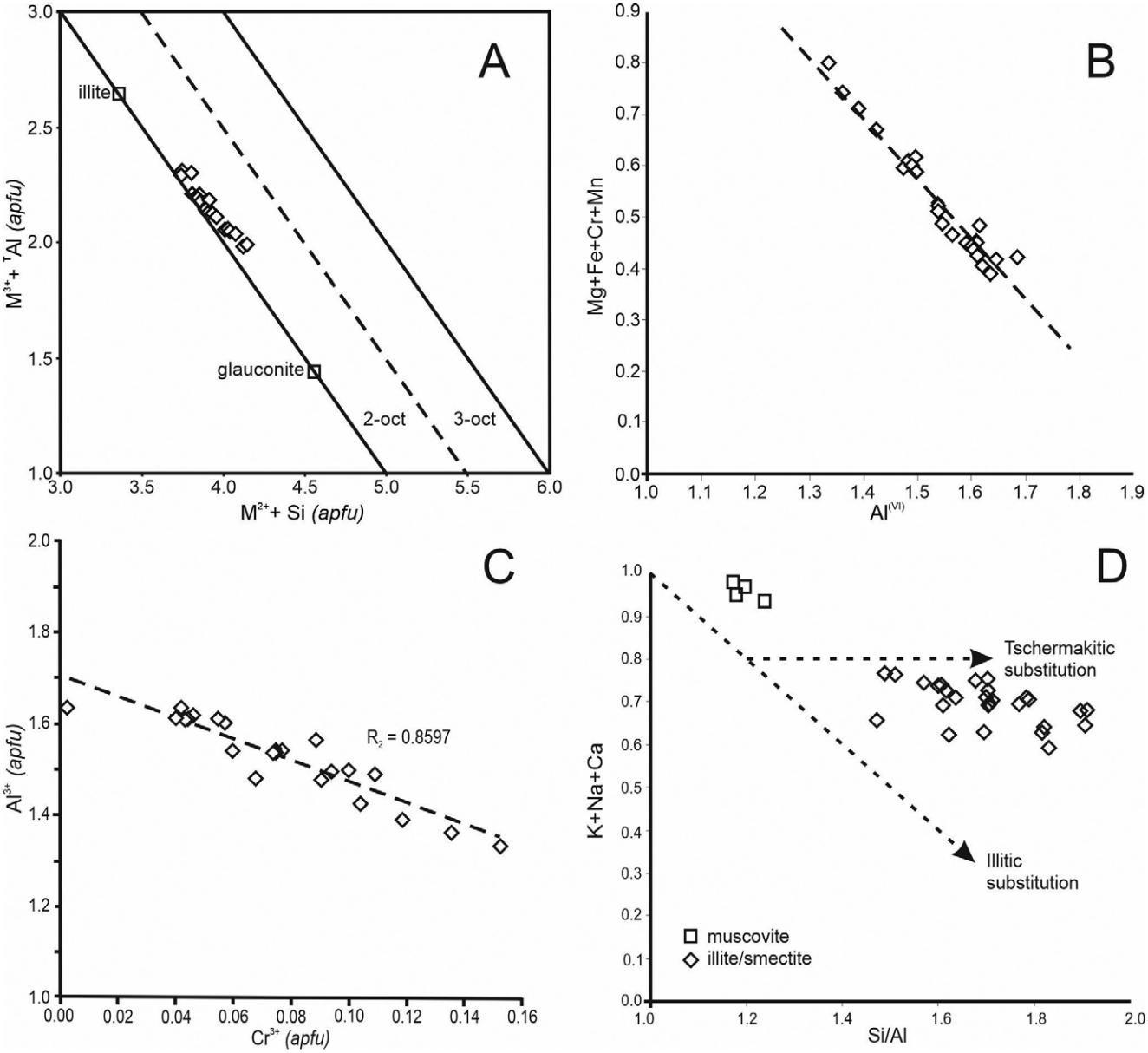

Fig. 5. Compositional variability of studied I/S. **A.** M^{2+}+ Si vs. M^{3+} + Al diagram. Representative illite and glauconite compositions are according to Rieder *et al.* (1998). The dashed line is the boundary between di- and trioctahedral micas (Ferenc *et al.*, 2016). **B.** Linear correlation Al^{VI} vs. (Mg + Fe + Cr + Mn) Randive *et al.* (2015). **C.** Correlation of Cr^{3+} and Al^{3+} in the octahedral position (Morata *et al.*, 2001). **D.** Si/Al vs. (K + Na + Ca) diagram showing dominant Tschermakitic substitution Randive *et al.* (2015).

Lower amounts of other minerals were also found in the fine (< 2 and < 5 μm) fractions: smectite, mica (or illite) in Havírna-Balinka and Nový Svět, kaolinite in Balinka, Oslavany and Moravský Krumlov and goethite in all samples except of Moravský Krumlov (Figs 6, 7; Suppl. Figs S1–S4). At Havírna-Balinka and Nový Svět, the smectite was identified on the basis of the (001) reflection, expanding upon EG solvation (Suppl. Figs S1, S2). Higher-order smectite reflections were not observed in the air-dried samples owing to low relative intensities and overlaps with I/S peaks.

No significant differences between the < 2 and < 5 μm fractions within the individual sites appeared (Suppl. Fig. S5). Only the non-clay minerals were somewhat higher in the < 5 μm fractions.

In the coarse > 5 μm fractions, variable percentages of other phyllosilicates and non-clay minerals were observed. These are mainly impurities; only chlorite occurs both in the green aggregate and in the surrounding rock. Quartz and mica or illite and goethite were identified in all samples. The mica content is the highest at Moravský Krumlov, where the (0 0 1) reflection may be clearly observed, despite the overlaps with I/S peaks. Plagioclase and K-feldspar are present in the Oslavany, Moravský Krumlov and Nový Svět samples. Except for Rakšice, carbonates (calcite predominates over dolomite) and chlorite are present in all samples. The highest chlorite percentage is developed in the Balinka sample. A low amount of kaolinite is found in the Rakšice sample. However, its presence in the other samples may not be excluded, owing to the overlap of (0 0 1) kaolinite with (0 0 2) chlorite reflection.

K-Ar dating of I/S

The K-Ar dates of the Oslavany and Rakšice <2 μm fractions are relatively consistent (Tab. 5). It is visible that only one melting by a defocused infrared laser was necessary to remove practically all radiogenic ^{40}Ar. The second melting contributed only <0.1% of the total radiogenic ^{40}Ar. Both ages are lower Permian: Oslavany is of Kungurian (284.1 ± 7.7 Ma), and Rakšice is of Kungurian/Artinskian (276.3 ± 7.4 Ma) age.

DISCUSSION

Lithology of the Balinka Conglomerate and depositional conditions

The fossil record indicates relatively humid climatic conditions of the Carboniferous sedimentation of the Balinka Conglomerate and the Rosice-Oslavany Formation (Šimůnek and Martínek, 2009; Opluštil *et al.,* 2016). Variable values of the chemical index of alteration (CIA; Nesbitt and Young, 1984) for the matrix of the Balinka Conglomerate (Houzar *et al*., 2013; Buriánek *et al.,* 2020; Hrdličková *et al*., 2020) from 33 to 58 indicate the rapid denudation by fluvial erosion rather than a variation in chemical weathering. The poorly sorted, coarse-grained Balinka Conglomerate is interpreted as the products of the mass flow in the alluvial fans (Nehyba *et al.,* 2012).

Variations in pebble petrography, pebble size and rounding, matrix content and the supply of material from local bedrock indicate transport over short distances. The chemical composition and petrography show that terrigenous clastic material in the Balinka Conglomerate was derived from the rapid erosion of adjacent crystalline units and their previous Palaeozoic cover, located to the west of the Boskovice Basin. The clasts of the Balinka Conglomerate were transported over relatively short distances from the Moldanubian Zone (Gföhl Unit, Svratka Crystalline Complex) and Moravosilesian Zone (Olešnice and Bíteš units) crystalline complexes by palaeorivers (e.g., Suess, 1907; Malý and Uhrová, 1980).

The chemical composition of the matrix of the Balinka Conglomerate with Cr-rich phyllosilicates (Houzar *et al.,* 2013) shows an elevated content of Cr (205 ppm) and Ni (48 ppm), compared to typical sandstones and conglomerates (chemical composition of the matrix) of the Boskovice Basin (32–103 ppm Cr and 9–35 ppm Ni; Buriánek *et al.,* 2020; Hrdličková *et al.,* 2020). The high Cr and Ni bulk contents indicate an abundance of ultramafic rocks in the source regions of the studied sediments (Garver *et al.,* 1996).

Cr-rich spinelides (Cr-spinel, magnesiochromite, chromite) are common accessory minerals in altered ultrabasic and basic rocks of Gföhl Unit of the Moldanubian zone adjacent to the Boskovice Basin (Fig. 8; Weiss, 1966; Medaris *et al.,* 2005, 2013; Hršelová *et al.,* 2018). Some authors

Table 5

Results of the K-Ar dating of two clay fractions of selected samples

Sample	% K_2O	Mass [mg]	% K	% ^{40}Ar*	Age	Error
Oslavany	6.93	13.26	5.753	91.1	276.1743	6.7273
				0.7	0.1093	0.6365
				SUM	276.28	7.36
Rakšice	6.78	10.55	5.628	92.0	283.7837	7.2005
				2.4	0.3070	0.4878
				SUM	284.09	7.69

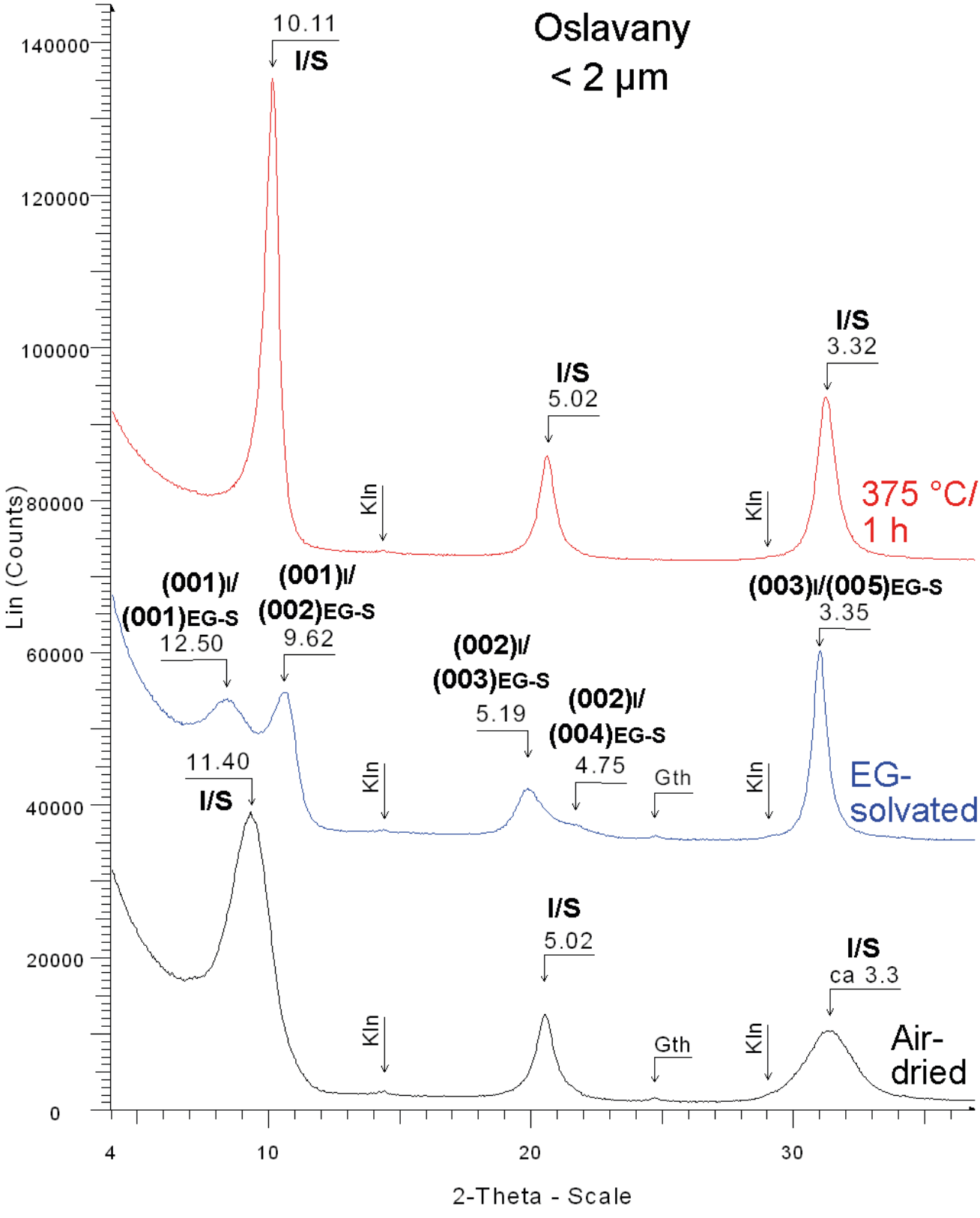

Fig. 6. Diffractograms (4–37 °2Θ) of air/dried, ethylene glycol solvated and 375 °C/lh heated oriented mounts of < 2 µm fraction of the Oslavany sample. Reflections of R1-illite(0.8)/smectite are marked in bold and d-values in Å are given for them. I/S – illite/smectite, Gth – goethite, Kln – kaolinite.

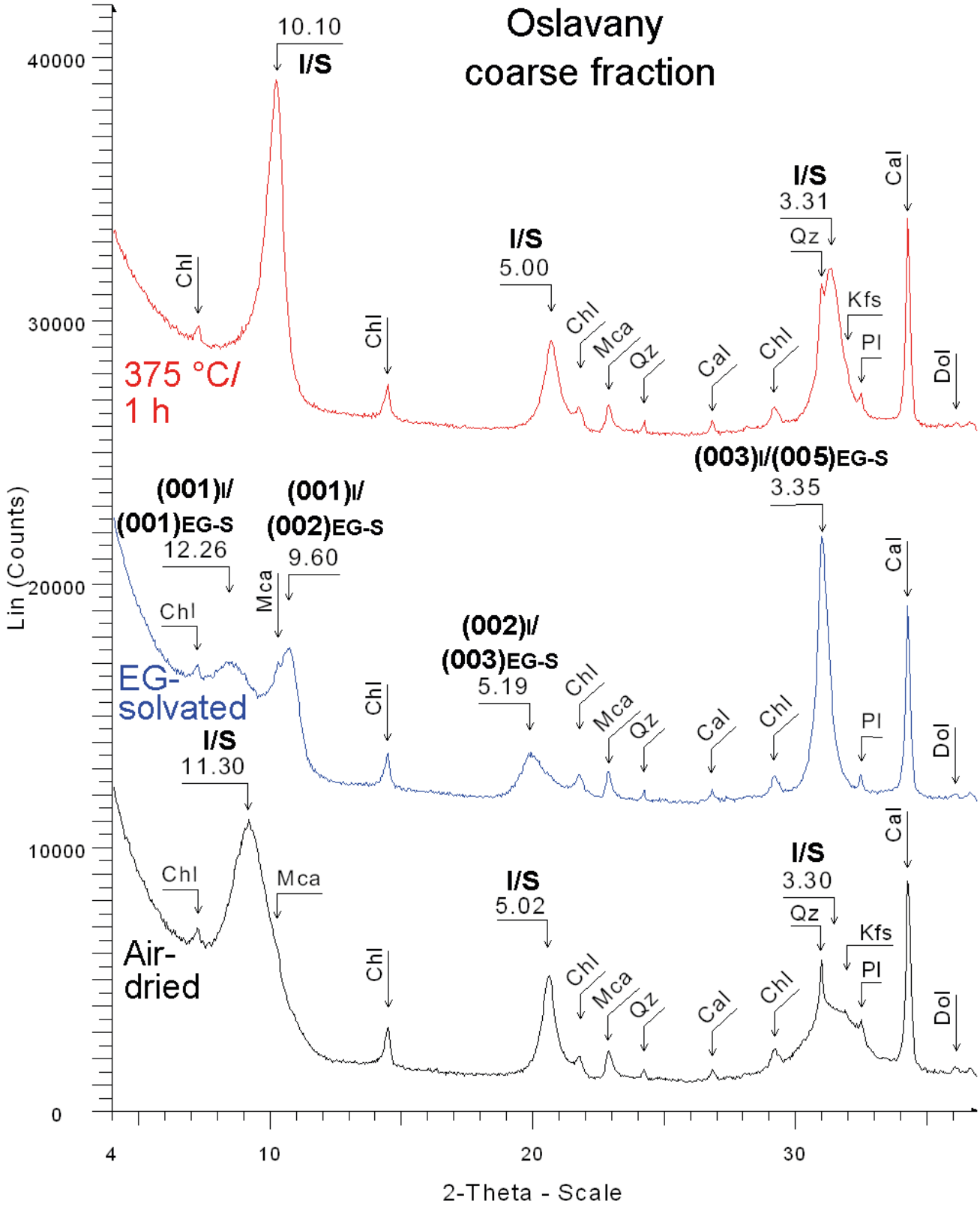

Fig. 7. Diffractograms (4–37 °2Θ) of air/dried, ethylene glycol solvated and 375 °C/1h heated oriented mounts of coarse > 5 μm fraction of the Oslavany sample. Reflections of R1-illite(0.8)/smectite are marked in bold and d-values in Å are given for them. Cal – calcite, Chl – chlorite, Dol – dolomite, I/S – illite/smectite, Kfs – K-feldspar, Pl – plagioclase, Mca – mica, Qz – quartz.

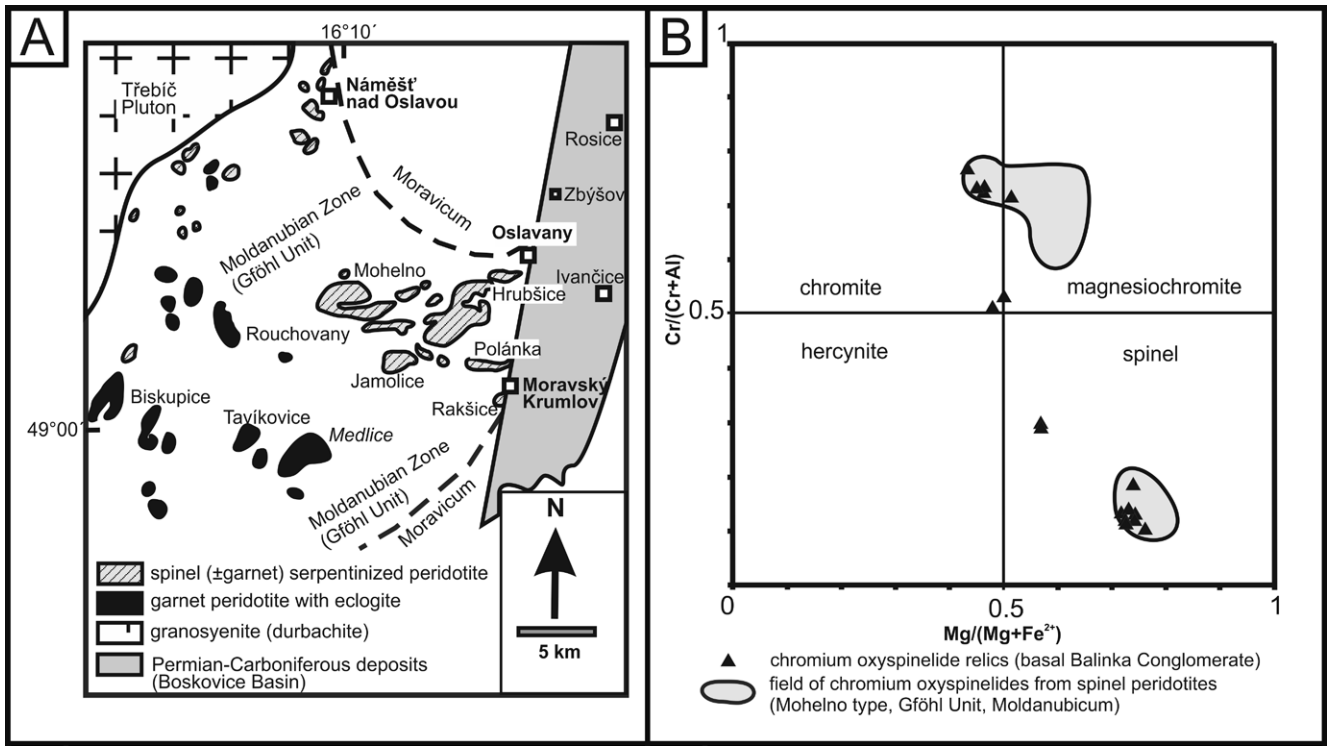

Fig. 8. Primary occurrence of spinels in the adjacent Moldanubian Zone and comparison of spinel chemistry in the Balinka Conglomerate. **A.** Serpentinite occurrences in Gföhl Unit surrounding the Boskovice Basin. Serpentinized spinel (±garnet) type is defined modified after Weiss (1966) and Medaris *et al.* (2013). **B.** Compositions of the chromium-bearing spinels in the heavy mineral assemblage of conglomerates in the Boskovice Basin and peridotites from the adjacent Gföhl Unit including two subtypes of spinel (±garnet) Mohelno type peridotites (see Medaris et al., 2005; Hršelová *et al.*, 2018, for explanations).It can be seen that, while magnesiochromite is common in peridotites, it is almost absent in the Balinka Conglomerate.

(Maksimovic and Brindley, 1980; Oze *et al.,* 2004) argued that Cr-rich spinelides are not a significant source of Cr, compared to silicates. However, in this case, chromium illite/smectite are always spatially associated with relics of the Cr-rich spinelides (Fig. 4). Therefore, the present authors interpreted chromium-rich phyllosilicate angular aggregates as the replacement products of spinel-rich serpentinized peridotites clasts in the conglomerates (Hršelová *et al.,* 2018). Relatively low content of Cr was reported from pyroxene and olivine in parental peridotites (up to 3 wt.% Cr_2O_3; Becker, 1997). Chromium-bearing green phyllosilicates, surrounding Cr-rich spinelides in source ultrabasic rocks, are absent (Medaris *et al.,* 2005). The smaller part of Cr-rich spinelides could also be generated by weathering of the Culmian greywackes and conglomerates partly underlying sediments of the Boskovice Basin in the south, which contain accessory chromium spinels (Čopjaková, 2007).

Diagenetic conditions and chromium illite/smectite genesis

The surfaces of the studied Cr-rich spinelides show signs of etching of variable intensity (Fig. 4A). The chemical composition of the spinels corresponds mainly to spinel and chromite, while magnesiochromite is very rare and hercynite is absent; 9.80–56.73 wt.% Cr_2O_3; 11.41–57.31 wt.% Al_2O_3; 10.75–20.50 wt.% FeO and 8.84–19.22 wt.% MgO; no zoning in spinels was observed (Hršelová *et al*., 2018). It can be seen that while magnesiochromite is common in peridotites, it is almost absent in the Balinka Conglomerate (Fig. 8). Also, garnet grains are affected by post-depositional dissolution and locally pyrope garnet (1.45–3.35 wt% Cr_2O_3) is rimmed by calcite. Rarely, also chromium-bearing I/S can fill their fractures and pores (Hršelová *et al.,* 2021).

In all the Balinka Conglomerate localities studied in the southern part of Boskovice Basin (see localities in Fig. 2), I/S is found in the form of angular aggregates in the conglomerate matrix and containing relics of Cr-rich spinelides. K/Ar dating of I/S shows that I/S is not transported from the primary ultrabasic rocks, but regarding age clearly diagenetic and Lower Permian. In the north part of the Rosice-Oslavany Sub-basin (Oslavany), the Balinka Conglomerate is lying below the Carboniferous–Permian boundary (Opluštil *et al.,* 2017) and the I/S sample yielded K-Ar age of 276.3 ± 7.4 Ma (Tab. 5). In Rakšice (south part of the Rosice-Oslavany Sub-basin), the data indicate the K-Ar age of 284.1 ± 7.7 Ma, but the age of sediments is not precisely determined there. However, according to lithostratigraphy (the same situation as in Oslavany, i.e., basal conglomerate in the bedrock underlying grey mudstones with a small layer of black coal), an Upper Carboniferous age is also very likely. Both datasets clearly prove that it is a diagenetic product of Permian age in the basal part of the basin.

On the basis of textural position, the chromium-rich I/S in the Balinka Conglomerate can be considered mostly

authigenic. The typical feature is its occurrence, restricted to relic chromium spinel and chromite, and it forms irregular aggregates (Fig. 4) in the fine-grained matrix, composed of clays, Cr-bearing chlorites Cr_2O_3 (≤ 2.92 wt.%) and carbonates. For this reason, the occurrence of these I/S can be used for lithostratigraphic correlation in BB.

Chromium-rich spinelides are relatively resistant heavy minerals. However, they can be affected by an incongruent dissolution during low-grade hydrothermal alteration, weathering and diagenesis, and Cr can be mobilized as Cr^{6+} ion (e.g., Hounslow 1996; Oze *et al.,* 2004; Garnier *et al.,* 2008). Hexavalent Cr migrates easily, especially if fluids contain CO_3^{2-}, SO_4^{2-}, Cl^- or organic compounds. In the reduced form, Cr^{3+} is preferentially absorbed to the Fe^{3+} oxides and only to a limited extent enters the phyllosilicates (e.g., Quantin *et al.,* 2002; Garnier *et al.,* 2008; Ajouyed *et al.,* 2011; Arai and Akizawa, 2014; Rosales *et al.,* 2017).

Chromium-rich phyllosilicates can be formed during the reaction of Cr-rich spinelides with clay-size silicates and metamorphic fluids (Kimball, 1990; Barnes, 2000; Barnes and Roeder, 2001; Oze *et al.,* 2004; Mellini *et al.,* 2005). Chromium-rich I/S is a relatively rare secondary mineral, which has been described only from geochemically specific environments, e.g., altered ultramafic rocks (Ferenc *et al.,* 2016, Belogub *et al*., 2017).

It is likely that chromium first may have been bound in smectite and during illitization (increase in Al, K and decrease in Fe, Mg, and Cr; Fig. 5) may also have entered illite (Tab. 2). Chromium can replace surface Al-octahedra by paired Cr^{3+} octahedra, incorporation of Cr^{3+} into the illite structure is also possible (Hao *et al*., 2022).

Illite could be formed in sedimentary basins from kaolinite and K-feldspar at temperatures ca. 150–200 °C (Cathelineau and Izquierdo, 1988; Ji and Browne, 2000; Lanson *et al.,* 2002; Inoue *et al.,* 2004). The illite content in the Balinka Conglomerate I/S of ca. 80%, which was estimated on the basis of the measured XRPD data and according to Moore and Reynolds (1997), corresponds to 110–130 °C by Horton (1985). But in the same work, a significantly higher temperature range (150–190 °C) indicated I-S with 80%. A higher temperature of ca. 180 °C of illitization, based on the 80% of illite in I-S, also was suggested in other works (Pollastro, 1993; Šucha *et al.,* 1993). Chromium-rich illite and mixed I/S are reported from low-grade metamorphic and hydrothermal *P-T* conditions of ≤ 0.5 kbar at ca. 130–160 °C, and > 0.5 kbar at ca. 200–300 °C (Maksimovic and Brindley, 1980; Higueras *et al.,* 1999; Morata *et al.,* 2001).

Temperatures of 215–230 °C were reported from vitrinite-reflectance measurements from the overlying coal-bearing Rosice-Oslavany formation of the southern part of the Boskovice Basin (Šafanda and Malý, 1994; Franců *et al*., 1998; Holzer, 2018). Owing to the assumed burial depth of the sediments (ca. 2.5–4.0 km), the conditions for the formation of the I/S lie on the border of diagenesis and hydrothermal processes in the Boskovice Basin (Franců *et al.*, 1998; Hršelová *et al.*, 2021). Small hydrothermal veins of calcite and barite occur in places in the studied conglomerates, but they completely lack I/S (Houzar and Hršelová, 2016). Volcanic rocks in the Boskovice Basin were affected by similar alteration, with homogenization temperatures of up to 128 °C and low- to moderate-salinity aqueous fluids (4–6 wt.% NaCl eq.). This hydrothermal alteration is probably temporally related to volcanic activity in the Boskovice Basin (Kratinová, 2009), which was dated directly at the Carboniferous/Permian boundary, i.e., 298.88 ± 0.09 Ma (Opluštil *et al.,* 2017).

Chromium-bearing chlorite is also present and is associated with the studied I/S. Its origin is not contradicted by the temperature conditions of the Balinka Conglomerate studied (Šafanda and Malý, 1994). Situations similar to the studied associations of chromium-bearing chlorite and I/S have also been reported in listvenites (Morata *et al.*, 2001; Randive *et al.*, 2015). Also, in this case, the formation of illite-smectite is interpreted as a polyphase process, where early hydrothermal alteration of the primary Cr-rich spinels produced Cr-rich chlorite and fuchsite. Subsequently, during the low-temperature second stage of alteration (270 °C), illite-smectite partially to completely replaced the Cr-rich chlorite and fuchsite (Morata *et al.*, 2001). Alternatively, Lanson *et al.* (2009) described the origin of the I/S and chlorite as several steps of smectite transformation, depending on the depth of burial at a low temperature.

CONCLUSIONS

This paper is focused on the mineralogical and structural characteristics of the lower part of the sedimentary sequence of the Boskovice Basin (eastern part of the Bohemian Massif). The occurrence of accumulations of green angular chromium phyllosilicates (several mm in diameter) is restricted to only the basal Balinka Conglomerate, underlying coal seams of the Rosice-Oslavany Sub-basin of the Upper Carboniferous. Textural evidence indicates that the Cr-rich phyllosilicates are products of the diagenetic transformation of Cr-rich oxyspinels and associated silicates (e.g., serpentine group) at temperatures of about ca. 110–190 °C, accompanied by K^+ activity, with Cr^{6+} in hydrothermal solutions. The dominant component of these accumulations of chromium-rich phyllosilicates is interstratified clay mineral R1-illite(0.8)/smectite (I/S). It is associated with carbonates (dolomite, calcite), anhedral (corroded) relics of Cr-rich spinelides, and Cr-rich chlorite rarely. Chromium I/S was formed mainly owing to the dissolution of Cr-rich spinelides (especially magnesiochromite).

The formation of clay chromium I/S was contemporaneous with elevated geothermal activity near the Carboniferous–Permian boundary (284.1 ± 7.7 and 276.3 ± 7.4 Ma).

Acknowledgements

This article appears through the institutional support of long-term conceptual development of research institutions, provided by the Ministry of Culture (ref. MK000094862) for PH and SH. Part of the work was also carried out with the support of CEITEC Nano Research Infrastructure (MEYS CR, 2016–2019). This is also a contribution to the Strategic Research Plan of the Czech Geological Survey (DKRVO/ČGS 2018-2022). Thanks go to

Radek Škoda and Petr Gadas for carrying out the EPMA analysis. The editors Bartosz Budzyń, Ewa Malata and Frank Simpson, the reviewer Martin Šťastný and two anonymous reviewers are acknowledged for their valuable comments that significantly improved the paper.

Supplementary material

Supplementary material related to this article is available at https://doi.org/10.14241/asgp.2023.05

REFERENCES

Abbott, A. N., Löhr, S. & Trethewy, M., 2019. Are clay minerals the primary control on the oceanic rare earth element budget? *Frontiers in Marine Science,* 6: 1–19.

Ajouyed, O., Hurel, C. & Marmier, N., 2011. Evaluation of the adsorption of hexavalent chromium on kaolinite and illite. *Journal of Environmental Protection*, 2: 1347–1352.

Arai, S. & Akizawa, N., 2014. Precipitation and dissolution of chromite by hydrothermal solutions in the Oman ophiolite: New behavior of Cr and chromite. *American Mineralogist,* 99: 28–34.

Barnes, S. J., 2000. Chromite in komatiites, II. Modification during greenschist to mid-amphibolite facies metamorphism. *Journal of Petrology*, 41: 387–409.

Barnes, S. J. & Roeder, P. L., 2001. The range of spinel composition in terrestrial mafic and ultramafic rocks. *Journal of Petrology*, 42: 2279–2302.

Becker, H., 1997. Petrological constraints on the cooling history of high-temperature garnet peridotite massifs in lower Austria. *Contributions to Mineralogy and Petrology*, 128: 272–286.

Belogub, E. V., Melekestseva, I. Y., Novoselov, K. A., Zabotina, M. V., Treťjakov, G. A., Zalykov, V. V. & Yuminov, A. M., 2017. Listvenite-related gold deposits of the South Urals (Russia): A review. *Ore Geology Reviews*, 85: 247–270.

Buriánek, D., Bubík, M., Franců, J., Fürychová, P., Havlín, A., Gilíková, H., Janderková, J. Konečný, F., Krejčí, Z., Krumlová, H., Kryštofová, E., Kunceová, E., Müller, P., Otava, J., Paleček, M., Pecina, V., Poul, I., Sedláček, J., Skácelová, Z., Šrámek, J., Petrová, P., Verner, K., Večeřa, J. & Vít, J., 2020. *Vysvětlivky k základní geologické mapě České republiky 1 : 25 000 list 24–341 Oslavany.* Závěrečná zpráva. Unpublished MS Česká geologická služba, Praha, 257 pp. [In Czech.]

Burley, S. D., Kantorowicz, J. D. & Waugh, B., 1985. Clastic diagenesis. *Geological Society London Special Publications*, 18: 189–226.

Cathelineau, M. & Izquierdo, G., 1998. Temperature – composition relationships of authigenic micaceous minerals in the Los Azufres geothermal system. *Contributions to Mineralogy and Petrology*, 100: 418–428.

Čepek, L., 1946. Tektonika Boskovické brázdy. *Věstník Státního geologického ústavu Československé republiky*, 20, 1–6: 128–130. [In Czech.]

Čopjaková, R., 2007. *The Reflection of Provenance Changes in the Psefitic and Psammitic Sedimentary Fraction of the Myslejovice Formation (Heavy Mineral Analysis).* Unpublished PhD Thesis, Masaryk University, Brno, 137 pp. [In Czech, with English summary.]

Deocampo, D. M., 2015. Authigenic clay minerals in lacustrine mudstones. *Special Paper of the Geological Society of America,* 515: 49–64.

Do Campo, N. & Nieto, F., 2005. Origin of mixed-layered (R1) muscovite-chlorite in an anchizonal slate from Puncoviscana Formation (Salta Province, Argentina). *Clay Minerals*, 40: 317–322.

Ferenc, Š., Uher, P., Spišiak, J. & Šimonová, V., 2016. Chromium- and nickel-rich micas and associated minerals in listvenite from the Muránska Zdychava, Slovakia: products of hydrothermal metasomatic transformation of ultrabasic rock. *Journal of Geosciences,* 61: 239–254.

Foord, E. E., Starkey, H. C., Taggart J. E., Jr. & Shawe, D. R., 1987. Reassessment of the volkonskoite-chromian smectite nomenclature problem. *Clays and Clay Minerals*, 35: 139–14.

Franců, J., Sýkorová, I., Franců, E., Šafanda, J. & Malý, L., 1998. Vitrinite reflectance and pyrolytic properties of coals in the Boskovice Furrow as related to thermal and burial history. In: Pešek, J., Opluštil, S. & Pešková, J. (eds), *Abstract VIII. Coal Geological Conference.* Charles University, Prague, 20 pp.

Garnier, J., Quantin, C., Guimaraes, E. & Becquer, T., 2008. Can chromite weathering be a source of Cr in soils? *Mineralogical Magazine*, 72: 49–53.

Garver, J. I., Royce, P. R. & Smick, T. A., 1996. Chromium and nickel in shale of the Taconic foreland: a case study for the provenance of fine-grained sediments with an ultramafic source. *Journal of Sedimentary Research*, 66: 100–106.

Hao, W., Chen, N., Sun, W., Mänd, K., Kirsimäe, K., Teitler, Y., Somelar, P., Robbins, L. J., Babechuk, M. G., Planavsky, N. J., Alessi, D. S. & Konhauser, K. O., 2022. Binding and transport of Cr(III) by clay minerals during the Great Oxidation Event. *Earth and Planetary Science Letters*, 584: 117503.

Havlena, V., 1964. *Geologie uhelných ložisek 2*. Československá akademie věd, Praha, 437 pp. [In Czech.]

Higueras, P., Oyarzun, R., Lunar, R., Sierra, J. & Parras, J., 1999. The Las Cuevas deposit, Almade´n district (Spain): Unusual case of deep-seated advanced argillic alteration related to mercury mineralization. *Mineraleralium Deposita,* 34: 211–214.

Holzer, P., 2018. *Model of depositional and erosional history of the Boskovice furrow*. Unpublished MSc. Thesis, Masaryk University, Brno, 49 pp. [In Czech, with English summary.]

Horton, D. G., 1985. Mixed-layer illite/smectite as a paleotemperature indicator in the Amethyst vein system, Creede district, Colorado, USA. *Contributions to Mineralogy and Petrology*, 91: 171–179.

Hounslow, M. W., 1996. Ferrimagnetic Cr and Mn spinels in sediments: Residual magnetic minerals after diagenetic dissolution. *Geophysical Research Letters*, 23: 2823–2826.

Houzar, S. & Hršelová, P., 2016. Research of Permo-Carboniferous sediments of the southern part of the Boskovice Graben; an overview (Part 1. History of Mining and Mineralogy). *Acta Musei Moraviae, Scientiae Geologicae*, 101: 3–32. [In Czech, with English summary.]

Houzar, S., Hršelová, P., Gilíková, H., Buriánek, D. & Nehyba, S., 2017. Research of Permian-Carboniferous sediments of the southern part of the Boskovice Graben; an overview (Part 2. Geology and Petrography). *Acta Musei Moraviae, Scientiae Geologicae,* 102: 3–65. [In Czech, with English summary.]

Houzar, S., Kopečná, P., Štelcl, J. & Vávra,V., 2013. Green chromium-bearing mica in Balinka Conglomerates of

Rosice-Oslavany Formation (Upper Carboniferous) at Oslavany. *Acta Musei Moraviae, Scientiae Geologicae*, 98: 3–12. [In Czech, with English summary.]

Hrdličková, K., Gilíková, H., Hanžl, P., Vít, J., Tomanová Petrová, P., Pecina, V., Buriánek, D., Večeřa, J., Kryštofová, E., Fürychová, P., Sedláčková, I., Baldík, V., Franců, J., Janderková, J., Kociánová, L., Kolejka, V., Konečný, F., Krejčí, O., Kunceová, E., Otava, J., Paleček, M., Sedláček, J., Šimůnek, Z., Dolníček, Z., Slobodník, M. & Šrámek, J., 2020. *Vysvětlivky k základní geologické mapě České republiky 1: 25 000, list 24–323 Veverská Bítýška.* Unpublished MS, Česká geologická služba, Praha, 265 pp. [In Czech.]

Hršelová, P., Houzar, S. & Buriánek, D., 2018. Chromium rich spinels of Upper Carboniferous Balinka Conglomerates from southern part of Boskovice Graben. *Acta Musei Moraviae, Scientiae Geologicae,* 103: 39–51. [In Czech, with English summary.]

Hršelová, P., Houzar, S. & Štelcl, J., 2021. Corroded garnets in the association of heavy minerals of Balinka conglomerates: their morphology and chemical compositon (Upper Carboniferous, Boskovice Basin). *Acta Musei Moraviae, Scientiae Geologicae,* 106: 35–50. [In Czech, with English summary.]

Inoue, A., Lanson, B., Fernandes, M., Sakharov, B., Murakami, T., Meunier, A. & Beaufort, D., 2005. Illite-smectite mixed-layer minerals in hydrothermal alteration of volcanic rocks: I. One-dimensional XRD structure analysis and characterisation of component layers. *Clays and Clay Minerals,* 53: 423–439.

Inoue, A., Meunier, A. & Beaufort, D., 2004. Illite-smectite mixed-layer minerals in felsic volcaniclastic rocks from drill cores, Kakkonda, Japan. *Clays and Clay Minerals*, 52: 66–84.

Jackson, M. L., 1979. *Soil chemical analysis – advanced course, 2nd Ed*. M. L. Jackson, Madison, WY, USA, 895 pp.

Jagodzinski, H., 1949. Eindimensionale Fehlordnung in Kristallen und ihr Einfluss auf die Röntgeninterferenzen. I. Berechnung des Fehlordnungsgrades aus den Röntgenintensitäten. *Acta Crystallographica,* 2: 201–207.

Jaroš, J., 1961. Geologický vývoj jižní části Boskovické brázdy. *Práce Brněnské základny ČSAV,* 32: 545–569. [In Czech.]

Ji, J. & Browne, P. R. L., 2000. Relationship between illite crystallinity and temperature in active geothermal systems of New Zealand. *Clays and Clay Minerals,* 48: 139–144.

Khoury, H. N., 2012. Long term analogue of carbonation in travertine from Uleimat quarries, central Jordan. *Environmental Earth Sciences,* 65: 1909–1916.

Khoury, H. N. & Al-Zoubi, A. S., 2014. Origin and characteristics of Cr-smectite from Suweileh area, Jordan. *Applied Clay Science*, 90: 43–52.

Kimball, K. L., 1990. Effects of hydrothermal alteration on the composition of chromian spinels. *Contribution to Mineralogy and Petrology*, 105: 337–346.

Kratinová, L., 2009. *The Alteration of Rocks of Boskovice Furrow – A Product of the Fossil Hydrothermal System?* Unpublished MSc Thesis, Masaryk University, Brno, 75 pp. [In Czech, with English summary.]

Králík, J. & Malý, L., 1987. Tufogenní horniny permokarbonu jižní části boskovické brázdy. In: Malý, L. (ed.), *Sborník III. konference Problematika geologické stavby uhelných ložisek ve velkých hloubkách*. ČSVTS, Zbýšov u Brna, pp. 96–101. [In Czech.]

Lanson, B., Beaufort, D., Berger, G., Bauer, A., Cassagnabere, A. & Meunier, A., 2002. Authigenic kaolin and illitic minerals during burial diagenesis of sandstones: a review. *Clay Minerals*, 37: 1–22.

Lanson, B., Sakharov, B. A., Claret, F. & Drits, V. A., 2009. Diagenetic smectite-to-illite transition in clay-rich sediments: A reappraisal of X-ray diffraction results using the multi-specimen method. *American Journal of Science*, 309: 476–516.

Maksimovic, Z. & Brindley, G. W., 1980. Hydrothermal alteration of a serpentinite near Takovo, Yugoslavia, to chromium-bearing illite/smectite, kaolinite, tosudite, and halloysite. *Clays and Clay Minerals*, 28: 295–302.

Malý, L., 1993. Formování sedimentační pánve permokarbonu boskovické brázdy a vývoj svrchnostefanské sedimentace v rosicko-oslavanské pánvi. In: Přichystal, A., Obstová, V. & Suk, M. (eds), *Geologie Moravy a Slezska: Sborník příspěvků k 90. výročí narození prof. dr. K. Zapletala.* Moravské zemské muzeum a Sekce geologických věd Přírodovědecké fakulty Masarykovy univerzity, Brno, pp. 8–99. [In Czech.]

Malý, L. & Uhrová, J., 1962. O slepencových souvrstvích v permokarbonu boskovické brázdy v rosicko-oslavanské pánvi. *Časopis Moravského muzea, Vědy přírodní*, 47: 53–58. [In Czech.]

Malý, L. & Uhrová, J., 1980. Příspěvek k paleogeografii karbonu v jižní části boskovické brázdy. *Časopis Moravského muzea, Vědy přírodní*, 65: 31–42. [In Czech.]

Manuella, F. C., Carbone, S. & Barreca, G., 2012. Origin of saponite-rich clays in a fossil serpentinite-hosted hydrothermal system in the crustal basement of the Hyblean Plateau (Sicily, Italy). *Clays and Clay Minerals*, 60: 18–31.

Medaris, L. G., Jr., Jelínek, E., Beard, B. L., Valley, J. W., Spicuzza, M. J. & Strnad, L., 2013. Garnet pyroxenite in the Biskupice peridotite, Bohemian Massif, anatomy of a Variscan high-pressure cumulate. *Journal of Geosciences,* 58: 3–19.

Medaris, L. G., Jr., Wang, H., Jelínek, E., Mihaljevič, M. & Jakeš, P., 2005. Characteristics and origins of diverse Variscan peridotites in the Gföhl Nappe, Bohemian Massif, Czech Republic. *Lithos,* 82: 1–23.

Mellini, M., Rumori, C. & Viti, C., 2005. Hydrothermally reset magmatic spinels in retrograde serpentinites, formation of "ferritchromit" rims and chlorite aureoles. *Contributions to Mineralogy and Petrology*, 149: 266–275.

Méring, J., 1949. L'Intéreference des rayons X dans les systems a` stratification dé sordonnée. *Acta Crystallographica*, 2: 371–377.

Mitsis, I., Godelitsas, A., Göttlicher, J., Steininger, R., Gamaletsos, P. N., Perraki, M., Abad-Ortega, M. M. & Stamatakis, M., 2018. Chromium-bearing clays in altered ophiolitic rocks from Crommyonia (Soussaki) volcanic area, Attica, Greece. *Applied Clay Science,* 162: 362–374.

Moore, D. M. & Reynolds, R. C., 1997. *X-Ray Diffraction and the Identification and Analysis of Clay Minerals*. Oxford University Press, Oxford, New York, 378 pp.

Morata, D., Higueras, P., Domínguez-Bella, S., Parras, J., Velasco, F. & Aparicio, P., 2001. Fuchsite and other Cr-rich phyllosilicates in ultramafic enclaves from the Almadén mercury mining district, Spain. *Clay Minerals,* 36: 345–354.

Nehyba, S., Roetzel, R. & Maštera, L., 2012. Provenance analysis of the Permo-Carboniferous fluvial sandstones of the southern

part of the Boskovice Basin and the Zöbing Area (Czech Republic, Austria): implications for paleogeographical reconstructions of the post-Variscan collapse basins. *Geologica Carpathica*, 63: 365–382.

Nesbitt, H. W. & Young, G. M., 1984. Prediction of some weathering trends of plutonic and volcanic-rocks based on thermodynamic and kinetic considerations. *Geochimica et Cosmochimica Acta*, 48: 1523–1534.

Odin, G. S., 1982. Interlaboratory standards for dating purposes. In: Odin, G. S. (ed.), *Numerical dating in stratigraphy*. Wiley and Sons, Chichester, UK, pp. 123–149.

Opluštil, S., Jirásek, J., Schmitz, M. & Matýsek, D., 2017. Biotic changes around radioisotopically constrained Carboniferous-Permian boundary in the Boskovice Basin (Czech Republic). *Bulletin of Geosciences*, 92: 95–122.

Opluštil, S., Schmitz, M., Cleal, J. Ch. & Martínek, K., 2016. A review of the Middle-Late Pennsylvanian west European regional substages and floral biozones, and their correlation to the Geological Time Scale based on new U-Pb ages. *Earth Science Reviews,* 154: 301–335.

Oze, C., Fendorf, S., Bird, D. K. & Coleman, R. G., 2004. Chromium geochemistry in serpentinized ultramafic rocks and serpentine soils from the Franciscan complex of California. *American Journal of Science*, 204: 67–101.

Pešek, J., 2004. *Late Paleozoic limnic basins and coal deposits of the Czech Republic*. Folia Musei rerum naturalium Bohemiae Occidentalis, Geologica, Suppl. 1, 188 pp.

Pešek, J., Holub, V., Jaroš, J., Malý, L., Martínek, K., Prouza, V., Spudil, J. & Tásler, R., 2001. *Geologie a ložiska svrchnopaleozoických limnických pánví České republiky*. Český geologický ústav, Praha, 243 pp. [In Czech.]

Pollastro, M. R., 1993. Considerations and applications of the illite/smectite geothermometer in hydrocarbon bearing rocks of Miocene to Mississippian age. *Clays and Clay Minerals*, 41: 119–133.

Pouchou, J. L. & Pichoir, F., 1985. "PAP" procedure for improved quantitative microanalysis. *Microbeam Analysis*, 20: 104–105.

Přichystal, A., 1993. Vulkanismus v geologické historii Moravya Slezska od paleozoika do kvartéru. In: Přichystal, A., Obstová, V. & Suk, M. (eds), *Geologie Moravy a Slezska: Sborník příspěvků k 90. výročí narození prof. dr. K. Zapletala.* Moravské zemské muzeum a Sekce geologických věd Přírodovědecké fakulty Masarykovy univerzity, Brno, pp. 59–70. [In Czech.]

Přichystal, A., 1994. Nové výskyty magmatických hornin v permu boskovické brázdy. *Geologické výzkumy na Moravě a ve Slezsku* v roce 1963(1): 60–62. [In Czech.]

Quantin, C., Becquer, T., Rouiller, J. H. & Berthelin, J., 2002. Redistribution of metals in a New Caledonia ferrelsol after microbial weathering. *Soil Science Society of America Journal Abbreviation*, 66: 1797–1804.

Randive, K., Korakoppa, M. M., Muley, S. V., Varade, A. M., 2015. Paragenesis of Cr-rich muscovite and chlorite in green-mica quartzites of Saigaon–Palasgaon area, Western Bastar Craton, India. *Journal of Earth Science,* 124: 213–225.

Rieder, M., Cavazzini, G., D'yakonov, Yu. S., Frank-Kamenetskii, V. A., Gottardi, G., Guggenheim, S., Koval', P. V., Müller, G., Neiva, A. M. R, Radoslovich, E. W., Robert, J.-L., Sassi, F. P., Takeda, H., Weiss, Z. & Wones, D. R., 1998. Nomenclature of the micas. *Canadian Mineralogist,* 36: 905–912.

Rosales, R. M., Faz, A., Gómez-Garrido, M., Munoz, A., Murcia, F. J., González, V. & Acosta, J. A., 2017. Geochemical speciation of chromium related to sediments properties in the riverbed contaminated by tannery effluents. *Journal of Soils and Sediments*, 17: 1437–1448.

Šafanda, J. & Malý, L., 1994. Paleogeothermal gradient in the Boskovice furrow. *Studia Geophysica et Geodaetica*, 38: 37–45.

Šimůnek, Z. & Martínek, K., 2009. Study of Late Carboniferous and Early Permian plant assemblages from the Boskovice Basin, Czech Republic. *Review of Palaeobotany and Palynology*, 152: 237–269.

Środoń, J., Zeelmaekers, E. & Derkowski, A., 2009. The charge of component layers of illite-smectite in bentonites and the nature of end-member illite. *Clays and Clay Minerals*, 57: 649–671.

Šucha, V., Kraus, I., Gerthofferová, H., Peteš, J. & Sereková, M., 1993. Smectite to illite conversion in bentonites and shales of the East Slovak Basin. *Clay Minerals*, 28: 243–253.

Suess, F. E., 1907. Die Tektonik des Steinkohlengebietes von Rossitz und Ostrand des böhmischen Grundgebirges. *Jahrbuch der Kaiserlich-Königlichen Geologischen Reichsanstalt*, 57: 793–834.

Taylor, T. R., Giles, M. R., Hathon, L. A., Diggs, T. N., Braunsdorf, N. R., Birbiglia, G. V., Kittridge, M. G., Macaulay, C. I. & Espejo, I. S., 2010. Sandstone diagenesis and reservoir quality prediction: Models, myths, and reality. *AAPG Bulletin*, 94: 1093–1132.

Weibel, R., Olivarius, M., Friis, H., Kristensen, L., Hjuler, M. L., Kjøller, C., Pedersen, P. K., Boyce, A., Mathiesen, A. & Nielsen, L. H., 2017. Climatic influence on early and burial diagenesis in Triassic and Jurassic sandstones from the Norwegian–Danish Basin. *The Depositional Record,* 3: 60–91.

Weiss, J., 1966. Ultrabasic rocks of the West Moravian Crystalline Complex. *Krystalinikum*, 4: 171–183.

Went, D. J., 2005. Pre-vegetation alluvial fan facies and processes: an example from the Cambro–Ordovician Rozel Conglomerate Formation, Jersey, Channel Islands. *Sedimentology*, 52: 693–713.

Whitney, D. L. & Evans, B. W., 2010. Abbreviations for names of rock-forming minerals. *American Mineralogist*, 95: 185–187.